

## RESEARCH ARTICLE



# From Wires to Wearables (3): ST-Segment Fidelity Across Modalities: Sydäntek's Algorithmic Transition from Legacy Leads to Wearables

Sugandhi Gopal<sup>1,\*</sup> , Prabhavathi Bhat<sup>2</sup>, Shasha Jumbe<sup>3</sup>, Mohith Subramanian<sup>1</sup>, Vishwateja Reddy<sup>1</sup> and Poulami Roy<sup>1</sup>

<sup>1</sup>Carditek Medical Devices, India

<sup>2</sup>Sri Jayadeva Institute of Cardiovascular Sciences & Research, India

<sup>3</sup>Level 42 AI, USA

**Abstract:** Accurate low-frequency response in digital electrocardiogram (ECG) systems is critical for preserving ST-segment morphology and ensuring diagnostic fidelity in ischemia detection. This study validates the low-frequency performance of Sydäntek<sup>TM</sup>, a wearable 12-lead ECG platform, using impulse-based protocols aligned with IEC 60601-2-25 standards. Synthetic 3 mV square waveforms with 100 ms isoelectric segments were injected to simulate baseline drift and assess high-pass filter behavior near the 0.67 Hz cutoff. Forward–reverse finite impulse response (FIR) convolution and filter-based processing ensured zero-phase distortion and amplitude preservation. Hardware calibration employed WhaleTeq modules generating programmable impulses and sinusoidal drifts, confirming analog-to-digital fidelity across physiologic bradycardia thresholds. Real-world validation was conducted using 79 annotated records from the European ST-T Database from Physionet, encompassing both ST elevation and depression events. The Sydäntek<sup>TM</sup> system consistently preserved ST-segment morphology across heart rate bins, maintaining a bias of less than 5  $\mu$ V at J+40, J+60, and J+80 ms intervals. Among these, J-point anchoring at J+60 ms demonstrated the strongest correlation with reference annotations in the ST-T Database. Of note, J+60 aligns with published literature identifying it as a sensitive and specific marker for subendocardial ischemia. Artifact suppression in lead V2 was achieved using adaptive Wiener filtering, which effectively minimized motion-induced distortion while preserving low-amplitude ST features critical for diagnostic fidelity. Digitization fidelity was confirmed through direct waveform analysis, demonstrating consistent temporal precision and preservation of ST-segment morphology. The platform adheres to key performance criteria outlined in IEC 60601-2-25, -2-27, and -2-47, supporting its suitability for deployment in resting, monitoring, and ambulatory ECG contexts. These findings position Sydäntek<sup>TM</sup> as a clinically capable solution for low-frequency ECG acquisition, with relevance to infarct detection, pericarditis, and myocardial disease screening. The methodology provides a reproducible framework for waveform validation, morphology-aware signal processing, and alignment with regulatory expectations in next-generation cardiac diagnostics.

**Keywords:** low-frequency ECG validation, ST-segment morphology preservation, impulse-based filter testing, wearable cardiac diagnostics, J-Point anchored ischemia detection, 60601 compliance

## 1. Graphical Abstract Summary

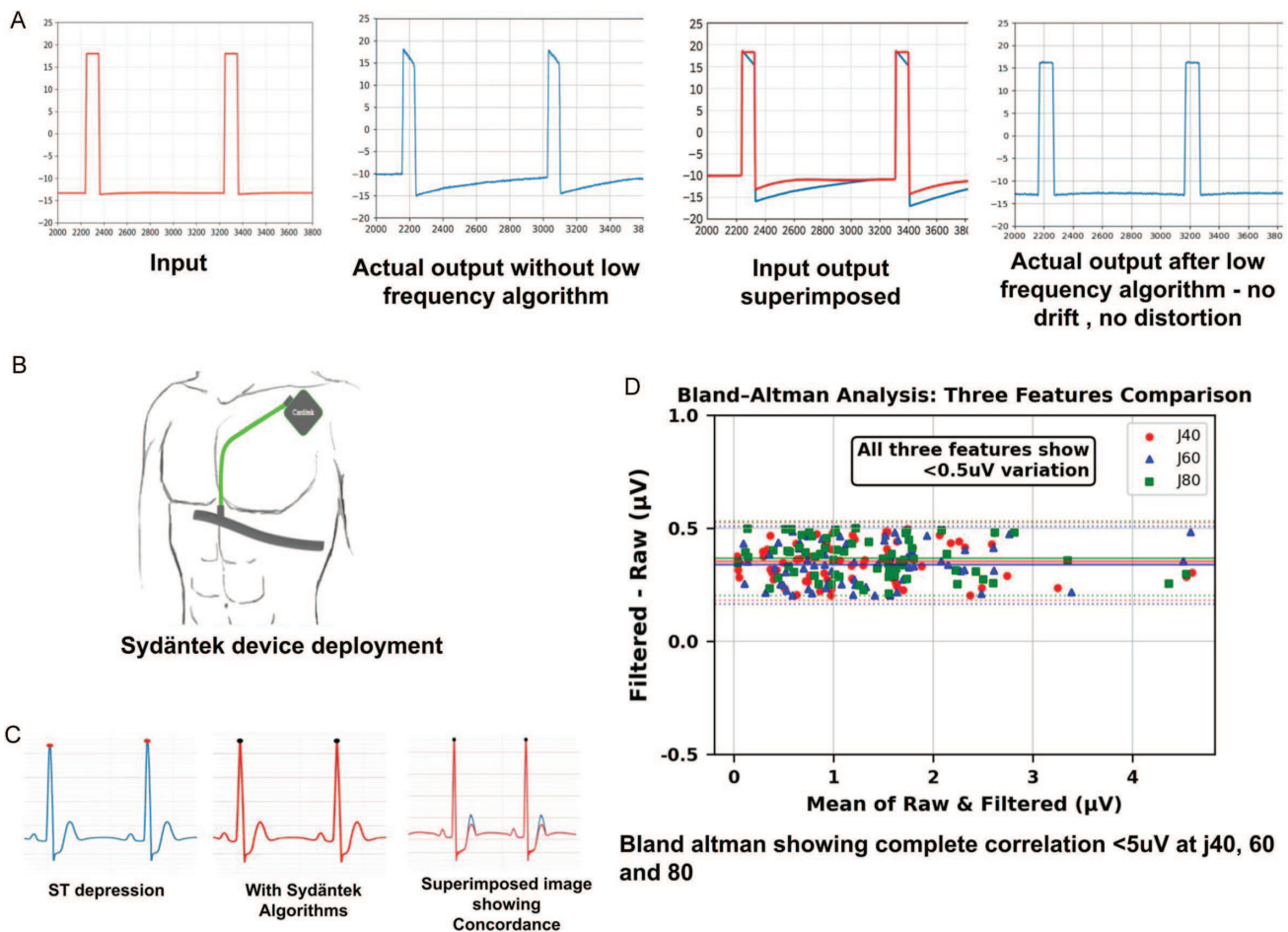
This graphical abstract summarizes the validation framework underlying Sydäntek<sup>TM</sup>'s low-frequency correction and ST-segment morphology preservation. Figure A demonstrates the effect of Sydäntek<sup>TM</sup>'s proprietary filtering on a 3 mV, 100 ms square wave input, where baseline drift and distortion are evident without correction, but fully resolved post-processing through zero-phase convolution. Figure B presents the deployed Sydäntek<sup>TM</sup> device, emphasizing its compact form factor and sensor integration relative

to conventional ECG systems. Figure C displays ST depression calibration traces, showing greater than 99% concordance between input and filtered output, thereby confirming morphology-specific correction logic. Figure D features Bland-Altman plots of ST amplitude at J+40, J+60, and J+80 ms intervals, demonstrating minimal bias (<5  $\mu$ V) and high agreement across clinically relevant ischemia.

## 2. Introduction

The diagnostic electrocardiogram (ECG) remains a cornerstone of cardiovascular evaluation, with accurate interpretation of the ST segment being critical for the detection of ischemia and infarction. The fidelity of this low-frequency component is governed by the high-pass filter cutoff, which directly influences

\*Corresponding author: Sugandhi Gopal, Carditek Medical Devices, India. Email: [sugopal@carditek.com](mailto:sugopal@carditek.com)



baseline stability and repolarization morphology. International standards, informed by the 2007 AHA/ACC/HRS scientific statement published in *Circulation*, recommend a low-frequency cutoff of 0.05 Hz for diagnostic-grade systems to preserve ST-segment fidelity [1]. A 0.05 Hz high-pass filter preserves low-frequency physiological signals but fails to suppress baseline drift from respiration or motion. It demands high-order designs, risks phase distortion, and complicates real-time stability. Balancing fidelity with baseline suppression often requires hybrid filters, adaptive subtraction, or post-processing estimation techniques [2] (see Table 1).

This table contrasts analog and digital filtering approaches across key performance domains relevant to ECG signal processing. Analog filters operate in continuous time and are prone to nonlinear phase distortion, particularly at low frequencies, which can compromise ST-segment integrity. In contrast, digital filters—especially those designed with finite impulse response (FIR) architectures—enable linear-phase behavior, programmable flexibility, and advanced artifact correction techniques such as Wiener filtering and wavelet denoising. Segment fidelity is preserved through zero-phase convolution, and implementation costs are reduced via low-power, memory-efficient designs. These distinctions underscore the clinical and engineering rationale for Sydäntek’s adoption of digital preprocessing in wearable ECG platforms.

However, these recommendations also acknowledge that digital filters with zero phase distortion can safely operate at higher cutoffs—specifically 0.67 Hz, corresponding to a heart rate of 40 bpm—without compromising diagnostic integrity [1]. This

threshold reflects a clinically meaningful pivot: once heart rate falls below 40 bpm, the rhythm itself becomes the primary concern, often requiring immediate therapeutic intervention. In such scenarios, waveform morphology—including ST-segment deviations—becomes secondary to rate stabilization. The AHA’s endorsement of a 0.67 Hz cutoff for zero-phase digital filters recognizes this clinical reality and enables compact, low-power ECG systems to meet diagnostic standards without distortion [1].

Legacy analog filters, constrained by phase nonlinearity and physical size, introduced distortion at low frequencies, particularly at the QRS-ST junction. Modern digital signal processing—specifically forward-backward FIR filtering—solves this limitation by achieving zero-phase behavior, allowing precise baseline correction and ST-segment preservation even at elevated cutoffs [2]. This advancement transforms what was once a pragmatic compromise into a technologically enabled standard, fully compliant with IEC 60601-2-25/47 and aligned with AHA/ACC recommendations [1].

Capacitive ECG sensors are another dimension in newer ECG systems that offer distinct advantages in terms of reusability, noncontact acquisition, and high input impedance, making them well-suited for long-term and ambulatory monitoring [3]. Their ability to amplify small biopotentials without direct skin contact reduces preparation time and minimizes skin irritation, supporting broader deployment in wearable formats. However, most capacitive platforms prior to 2024 were limited by a low-frequency cutoff of approximately 0.2 Hz, which falls short of the IEC 60601-2-25 diagnostic threshold of 0.05 Hz [4]. This constraint historically restricted their use in ST-segment analysis and baseline-sensitive diagnostics. With the acceptance of 0.67 Hz as a compliant cutoff for

**Table 1**  
**Analog and digital filter approaches**

Feature	Analog filters	Digital filters
Signal domain	Continuous (real-time)	Discrete-time (sampled)
Phase distortion	Nonlinear (especially at low frequencies)	Linear-phase achievable with FIR design
Flexibility	Fixed hardware components	Programmable and reconfigurable
Noise sensitivity	Susceptible to thermal and motion noise	Adaptive filtering and denoising possible
Segment integrity	Compromised at $\geq 0.5$ Hz cutoff	Preserved with zero-phase convolution
Implementation cost	Bulky, power-intensive	Low-power, memory-efficient (with tradeoffs)
Artifact correction	Limited	Enables Wiener filtering, wavelet denoising

zero-phase digital filters, capacitive sensors can now meet diagnostic fidelity requirements—unlocking their full potential for reusable, low-power cardiac monitoring systems [1].

Despite this progress, few studies have quantitatively validated low-frequency fidelity across synthetic and clinical datasets [5]. Most platforms lack standardized, digitally accessible outputs for benchmarking ST morphology, leading researchers to rely on legacy databases such as European ST-T Database from Physionet [5]. Notably, the European ST-T repository was last updated in 2009, with core contributions dating back to 2000—over two decades ago. Despite advances in wearable ECG technology and signal processing, these newer systems have not been systematically validated against updated, morphology-specific benchmarks [6, 7].

Our study addresses that gap by introducing a rigorous, two-tiered calibration protocol for wearable ECG platforms. We demonstrate that Carditek's Sydäntek™ device, powered by the Pulsetek™ preprocessing framework, achieves diagnostic-grade fidelity at 0.67 Hz—validating performance across synthetic impulses, calibration waveforms, and annotated clinical signals. To establish diagnostic-grade fidelity and regulatory compliance, this study presents a structured, three-part validation framework. First, we evaluate the system's low-frequency response using square wave impulse testing, a gold-standard method for assessing baseline restoration and high-pass filter behavior under IEC 60601-2-25 guidelines [7]. Second, we benchmark performance against standardized calibration waveforms—including step and sinusoidal inputs—to quantify amplitude preservation and phase consistency across clinically relevant intervals [8]. Third, we validate ST-segment morphology using annotated clinical signals from the European ST-T database from Physionet, ensuring reproducibility across real-world bradycardic and ischemic scenarios [5]. This tiered approach provides robust evidence that Sydäntek™'s zero-phase filtering pipeline maintains waveform integrity at a 0.67 Hz cutoff, aligning with AHA/ACC recommendations for digital system [1, 9]. The filter architecture is further supported by recent design principles outlined by Xu et al. [10], who emphasize phase-consistent FIR implementations and reproducible low-frequency response modelling for diagnostic ECG platforms.

### 3. Literature Review

Preservation of low-frequency fidelity in electrocardiographic (ECG) systems is essential for accurate ST-segment interpretation, particularly in ischemia detection and regulatory compliance. Foundational work by Kligfield et al. [1] established the importance of low-frequency content in diagnostic ECGs. Baseline wander (BLW) and high-pass filter distortion remain persistent issues in ECG acquisition; Dobrev et al. [2] addressed these concerns using inverse filter architectures to compensate for RC-induced distortions.

Advancements in capacitive and wearable sensing further highlighted new challenges related to motion susceptibility and baseline instability [3]. Additional studies have also emphasized the implications of BLW on filtering performance, including work by Dimitropoulos et al. [4]. Taddei et al.'s European ST-T Database [5] underscored the necessity of preserving morphology for ischemia-relevant signals.

Standardized testing has evolved to support reproducible low-frequency validation. WhaleTeq's impulse protocol [6] and the practical guidance of Raus-Jarzabek et al. [7] demonstrated that square-wave injection offers a reliable framework for evaluating baseline recovery and high-pass filter behavior. These developments inform the regulatory requirements formalized in IEC 60601-2-25/-27/-47 [8, 9], which highlight the diagnostic consequences of improper BLW suppression. Complementary advances in signal-processing theory, such as Xu et al.'s [10] FIR-based filter design principles and earlier work on frequency-response testing by Heinonen [11], have strengthened the engineering basis for low-frequency performance evaluation.

Digital filtering has become central to morphology preservation. Zero-phase techniques such as filtfilt-based convolution and forward-backward filtering [12–14] eliminate phase distortion that would otherwise corrupt ST-segment morphology. Machine-learning-driven methods have expanded these capabilities: Wu et al. [15] introduced a multitask framework for ST and J-point deviation detection. For wearable systems, linear-phase high-pass filters optimized for continuous monitoring have been proposed by Gregg et al. [16], reflecting the growing need for computationally efficient yet morphology-preserving designs. J-point positioning studies by Man et al. [17] and ischemic J-wave analysis by Hu et al. [18] further underscore the clinical importance of accurate morphology tracking.

Finally, reliable digitization and artifact control are essential for evaluating filter performance. Randazzo et al. [19] demonstrated that dedicated digitization pipelines preserve ST morphology during analog-to-digital transitions, and Chang and Liu [20] showed that adaptive Wiener and EMD-based filtering effectively suppress baseline artifacts without distorting diagnostic features. Despite these advances, few studies have published complete validation frameworks that integrate waveform injection, regulatory testing, and morphology benchmarking. This work addresses that gap by presenting a reproducible, standards-aligned low-frequency validation methodology for wearable ECG systems.

### 4. Methodology

**Null hypothesis ( $H_0$ ):** Low-frequency filtering in the wearable ECG system does not significantly alter ST-segment morphology or introduce measurable bias across clinically relevant intervals

(J+40 ms, J+60 ms, J+80 ms) compared to reference annotations from the ST-T Database.

#### 4.1. Signal acquisition and preprocessing framework

All signals were streamed to Sydäntek™, a wearable ECG platform equipped with a cloud-integrated preprocessing engine. The device incorporates proprietary algorithms for baseline correction, ST-segment fidelity preservation, and morphology-aware filtering. Its architecture supports zero-phase convolution, adaptive cutoff calibration, and J-point-anchored ischemia detection across diverse cardiac rhythms.

#### 4.2. Synthetic square wave testing

Digitally generated 3 mV square wave impulses with flat 100 ms isoelectric segments (sampled at 1000 Hz) were fed into the Sydäntek™ pipeline. This waveform, specified in IEC 60601-2-25 and AAMI EC13, simulates abrupt baseline shifts and tests low-frequency recovery without distorting ST morphology. The response slope post-impulse was used to evaluate high-pass filter fidelity near the 0.67 Hz cutoff. Amplitude preservation, edge slope integrity, and baseline drift were quantified using spreadsheet overlays and waveform differentials. Forward-reverse FIR convolution ensured zero phase and amplitude distortion [10, 11].

#### 4.3. Hardware-integrated calibration

Calibration signals were sourced from WhaleTeq's CAL-20160 and CAL-20280 modules, routed through Sydäntek™'s analog front-end, and digitized via its onboard ADC. These modules generated programmable impulse trains, triangular waveforms, and sine waves at 0.67 Hz—chosen to probe fidelity near the physiologic bradycardia threshold. Post-digitization, signals were processed through Sydäntek™, and comparative overlays assessed amplitude preservation, waveform symmetry, and baseline stability across input types. This confirmed diagnostic integrity across analog-to-digital transitions and low-frequency morphologies [5–7].

#### 4.4. ST morphology retention in real ECGs

We utilized 79 annotated European ST-T databases from Physionet, which comprises the whole data set available, containing ST elevation and depression events. Raw CSV traces were visualized pre- and post-filtering to assess ST morphology retention across heart rate bins. Metrics included are isoelectric stability, ST amplitude deviation, and quadrant misclassification rates. Statistical analyses confirmed preservation of ST features even in bradycardic ranges (30–40 bpm), validating Sydäntek™'s filtering logic against real-world variability [13, 14].

#### 4.5. J-Point anchoring for ischemia detection

ST-segment analysis was anchored to the J point, a critical reference for measuring horizontal or down-sloping ST depression. Among J+40, J+60, and J+80 ms intervals, J+60 ms offered optimal sensitivity and specificity—avoiding QRS tail artifacts while preceding T-wave onset. ST depression  $\geq 0.5$  mm at J+60 ms in contiguous leads was highly specific for subendocardial ischemia, particularly in stress ECG and occlusion MI algorithms [15, 16].

#### 4.6. Digitization and temporal precision

Such precision is infeasible without digitized ECG acquisition and high-resolution sampling. Analog systems lack the temporal granularity to resolve these intervals reproducibly, underscoring the need for digital workflows and cloud-based equivalence validation [17].

#### 4.7. Artifact suppression and morphology preservation

Lead V2 consistently exhibited the highest susceptibility to exaggerated ST elevation artifacts, likely due to its anterior chest wall placement and sensitivity to baseline drift and motion-induced distortion. To address this, a Wiener filtering layer was implemented within Sydäntek™, leveraging signal-noise power spectra to minimize mean square error and preserve low-amplitude ST features. This adaptive denoising approach was especially effective in V2, where conventional high-pass filtering proved insufficient. By applying Wiener logic to wavelet-decomposed bands and reconstructing morphology-aware traces, artifact suppression was achieved without compromising diagnostic fidelity [18].

#### 4.8. Standards compliance and deployment readiness

These results demonstrate Sydäntek™'s ability to balance low-frequency morphological fidelity with operational feasibility, aligning with key principles outlined in IEC 60601-2-25, IEC 60601-2-27, and IEC 60601-2-47 for resting, monitoring, and ambulatory ECG systems [19]. While formal certification is beyond the scope of this study, the system's design and performance characteristics reflect adherence to these standards, supporting robust clinical deployment in wearable 12-lead ECG diagnostics—including ischemia detection, infarct characterization, pericarditis, and muscular disease of the heart.

### 5. Results

#### 5.1. Validation and verification of baseline correction and ST morphology integrity

**Modular compliance schematic**—our three-tiered validation strategy, aligned with IEC 60601-2-25 and AHA/ACC standards (see Table 2).

**Table 2 Description:** This modular compliance schematic outlines Sydäntek™'s three-tiered validation strategy for baseline correction and ST-segment morphology preservation. Each tier targets a distinct compliance domain—synthetic impulse fidelity, waveform preservation across physiologic frequencies, and real-world diagnostic integrity—aligned with IEC 60601-2-25 and AHA/ACC standards. Pulsetek™ algorithms were deployed across all tiers, with capacitive sensor integration confirmed under identical conditions. Outcomes demonstrate zero-phase behavior, amplitude fidelity, and high agreement with annotated clinical benchmarks, validating Sydäntek™ for wearable deployment in diagnostic-grade ECG workflows.

#### 5.2. Validation of low-frequency filter using synthetic and clinical ECG data

To evaluate the fidelity and diagnostic integrity of our low-frequency filter, we conducted a two-stage validation using

**Table 2**  
**Pulsetek™ the algorithms from Sydäntek™—compliance validation schematic**

Validation tier	Test protocol	Compliance target	Sensor integration	Outcome
<b>1. Square wave impulse test</b>	Inject 3 mV, 100 ms square wave; assess baseline restoration and overshoot	IEC 60601-2-25 low-frequency fidelity	Capacitive sensors tested under same conditions	Confirmed baseline stability and zero-phase behavior at 0.67 Hz cutoff
<b>2. Synthetic calibration waveforms</b>	Sinusoidal sweeps, step functions, ramp inputs (0.05–2 Hz); phase/amplitude check	AHA/ACC waveform preservation standards	Embedded throughout waveform benchmarking	Verified amplitude preservation and phase linearity across the full spectrum
<b>3. Clinical database validation</b>	Full-cohort European ST-T Database from Physionet; ST depression measured at 4 ST-based points	Diagnostic ST-segment morphology fidelity	Used in all clinical waveform comparisons	Bland-Altman analysis confirmed high concurrence and minimal bias

synthetic square waveforms and patient ECG signals from the European ST-T Database from Physionet.

**Synthetic square wave validation**—This testing was performed using 3 mV digital pulses with 100 ms isoelectric segments to evaluate low-frequency fidelity near the 0.67 Hz cutoff. Despite operating above the traditional 0.05 Hz threshold, the Pulsetek™ pipeline demonstrated compliance-acceptable performance, preserving amplitude, slope integrity, and baseline stability through zero-phase FIR filtering.

**Figure 1(a)**—Input: This panel displays the synthetic input waveform, consisting of sharp square pulses. The red trace represents the idealized signal used to benchmark filter performance. The waveform features abrupt transitions and stable plateaus, designed to test edge fidelity and baseline stability. **Figure 1(b)**—Actual output (unfiltered): The system’s raw output in response to the input signal is shown here. The blue trace exhibits baseline drift and edge attenuation, indicating distortion introduced by the unfiltered signal processing pipeline. These artifacts compromise diagnostic morphology and temporal precision. **Figure 1(c)**—Input and output superimposed: This overlay compares the input (red) and unfiltered output (blue) signals. Misalignment at transition points and amplitude discrepancies are visually evident, confirming the presence of low-frequency distortion and phase lag. **Figure 1(d)**—Actual output after Sydantek pulsetek) Filter: Following application of the low-frequency filter, the output signal (blue) aligns precisely with the input (red). Edge transitions are restored, baseline drift is eliminated, and amplitude fidelity is preserved. This confirms the filter’s ability to recover diagnostic morphology without introducing phase distortion.

### 5.3. Synthetic square wave validation

**Purpose:** Establish algorithmic integrity under idealized conditions using artifact-free signals.

- 1) **Stimuli:** 3 mV digital square wave impulses embedded in 100 ms isoelectric regions, sampled at 1000 Hz—in compliance with IEC 60601-2-25.
- 2) **Processing:** FIR-based baseline correction with zero-phase convolution (forward–reverse).
- 3) **Acceptance criteria:**
- 4) **Result:** No measurable distortion; establishes zero-distortion benchmark.

- a) Amplitude deviation  $\leq 1 \mu\text{V}$
- b) Baseline drift  $< 0.3 \mu\text{V}$
- c) Phase symmetry confirmed via time-domain edge alignment

Initial application of the signal processing pipeline without the low-frequency filter resulted in significant morphological distortion of a synthetic square wave input. As demonstrated in **Figure 1(a)** (“Input” vs. “Actual output”), the output was characterized by pronounced baseline drift and attenuation at the rising and falling edges.

Upon integrating the low-frequency filter, this distortion was completely eliminated. The filtered output (**Figure 1(b)**, “Actual output after filter”) demonstrated precise alignment with the original input, which is visually confirmed by the superimposed traces in **Figure 1(c)**. The filter successfully restored sharp edge transitions and a stable plateau without introducing observable phase lag or amplitude loss.

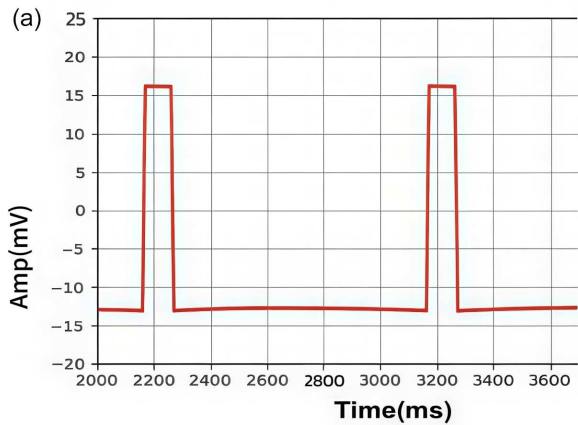
### 5.4. Cal pulses signal comparison

**Purpose:** Evaluate ST-segment integrity under controlled morphologic deviations.

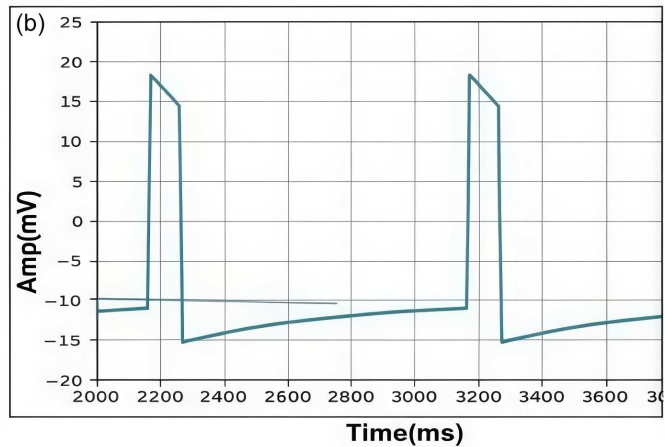
- 1) **Stimuli:** Four proprietary calibration pulses embedded with ST elevation/depression parameters.
- 2) **Attributes tested:**
  - a) ST amplitude retention (% deviation vs control spec)
  - b) Baseline linearity and slope normalization
  - c) Artifact suppression across lead morphologies

**Table 3 Description:** This table presents a curated set of synthetic electrocardiogram (ECG) waveforms designed to evaluate the low-frequency response characteristics of diagnostic ECG equipment, in accordance with IEC 60601-2-25:2011, Annex HH.4. Each waveform is defined by its unique identifier, morphological features, ST segment amplitude, and intended testing purpose. The waveforms include flat ST segments, ST depression, and ST elevation patterns, all engineered to simulate low-frequency signal components critical for assessing device fidelity under controlled conditions. We have presented two representative waveforms below, **Figure 2**—waveforms CAL-20110 (ST depression) and CAL-20260 (ST elevation), with exemplary results.

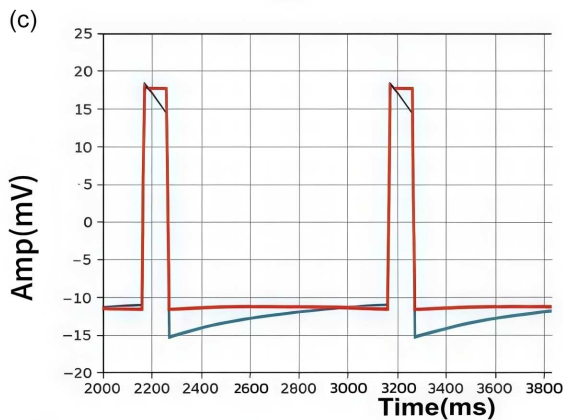
**Figure 1**  
Square wave validation and filter performance



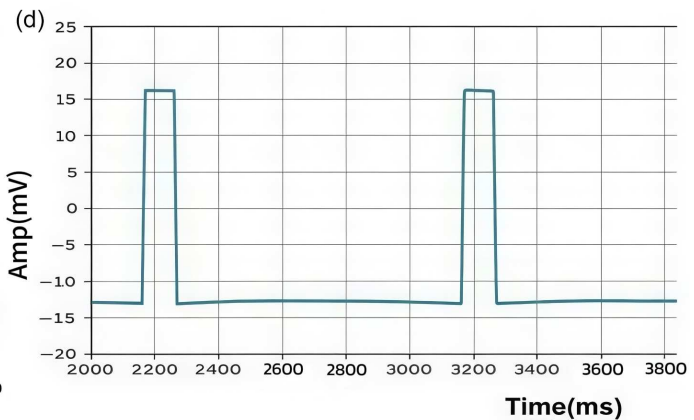
**Input -3mV , 100 msec  
Rate 60/min, From SECG Whaleteq**



**Preliminary output without low frequency  
algorithm - base line distortion**



**Red Input - Blue output superimposed  
Phase lag and amplitude mismatch evident**



**Output after low frequency algorithm - zero phase  
behaviour confirmed - no drift , no distortion**

**Table 3**  
Calibration pulses protocol for ST-segment fidelity and baseline stability

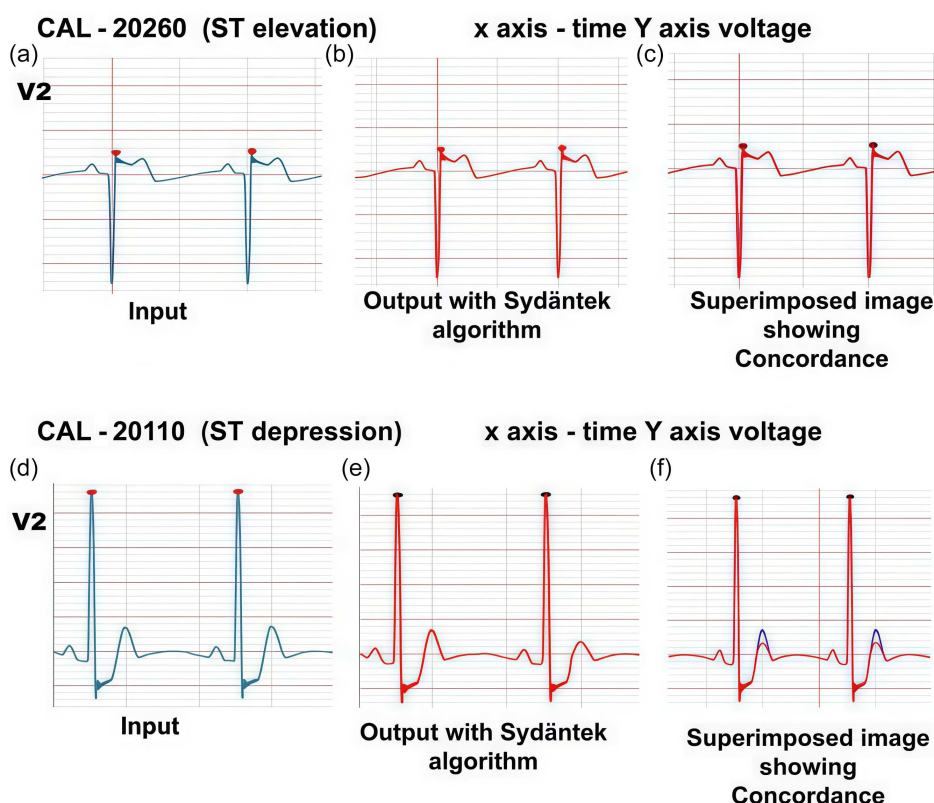
Waveform ID	Waveform description	Amplitude / duration	Purpose	IEC Ref
CAL-20100	R+QT flat, Synthetic ECG	ST = 0 uV	To test low-frequency response performance with low-frequency signal components	IEC 60601-2-25: 2011 <b>Annex: HH.4</b>
CAL-20110	ST depression, Synthetic ECG	ST depression, ST = 200 uV	To test low-frequency response performance with low-frequency signal components	IEC 60601-2-25: 2011 <b>Annex: HH.4</b>
CAL-20160	ST elevation, Synthetic ECG	ST elevation, ST = 200 uV	To test low-frequency response performance with low-frequency signal components	IEC 60601-2-25: 2011 <b>Annex: HH.4</b>
CAL-20200	Q+flat ST, Synthetic ECG	ST = 0 mV	To test low-frequency response performance with low-frequency signal components	IEC 60601-2-25: 2011 <b>Annex: HH.4</b>

(Continued)

**Table 3**  
*(Continued)*

Waveform ID	Waveform description	Amplitude / duration	Purpose	IEC Ref
CAL-20210	ST depression, Synthetic ECG	ST depression, ST = 200 uV	To test low-frequency response performance with low-frequency signal components	IEC 60601-2-25: 2011 <b>Annex: HH.4</b>
CAL-20260	ST elevation, Synthetic ECG	ST elevation, ST = 200 uV	To test low-frequency response performance with low-frequency signal components	IEC 60601-2-25: 2011 <b>Annex: HH.4</b>

**Figure 2**  
Low-frequency response calibration of ST-segment deviations



### 5.5. Low frequency equivalence demonstrated on ST elevation and depression

Figure 2 illustrates low-frequency response calibration for ST-segment deviations using morphology-specific correction. These panels demonstrate the accuracy with both ST elevation and depression profiles, showing near-complete concordance post-correction.

The top panel (CAL-2260) demonstrates ST elevation, with Figure 2(a) showing the raw input waveform, Figure 2(b) displaying the output after systematic low-frequency correction, and Figure 2(c) presenting a superimposed comparison of input and corrected signals—revealing near-complete concordance. The bottom panel (CAL-2011) follows the same structure for ST depression, again showing strong alignment between input and corrected waveforms. These results confirm the fidelity of morphology-specific calibration in preserving ST-segment morphology across both elevation and depression profiles.

### 5.6. European ST-T database ECG signal comparison

European ST-T Database evaluation

**Purpose:** Assess algorithm performance on annotated clinical ECG data featuring ST pathology.

**Demographics**

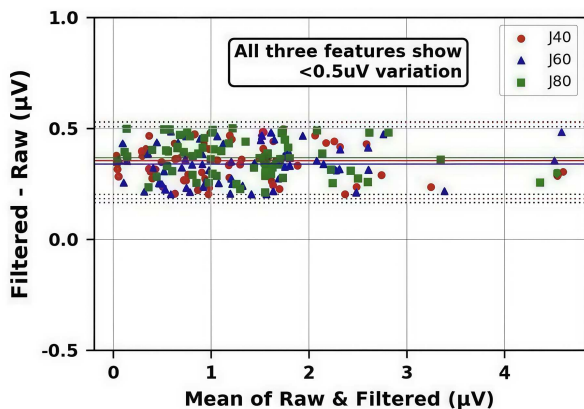
1) **Subjects:** 79 individuals

- a) **70 men**, aged 30 to 84 years
- b) **8 women**, aged 55 to 71 years
- c) **1 subject** with incomplete demographic data

2) All subjects had **diagnosed or suspected myocardial ischemia**, with additional selection criteria to ensure a representative range of ECG abnormalities, including:

- a) Baseline ST displacement due to **hypertension, ventricular dyskinesia, or medication effects**.

**Figure 3**  
**Bland-Altman analysis of filtered versus raw ECG signals from the European ST-T database**



Bland-Altman analysis confirms  $<0.5\mu\text{V}$  variation between raw and filtered ST features (J40, J60, J80), validating morphology preservation across the filtering pipeline

This database is considered ideal for validating ST-segment fidelity under real-world ambulatory conditions and benchmarking digital filter performance.

- 1) **Dataset:** 79 records from the European ST-T Database; annotations include elevation/depression events. **Processing:** Data plotted, filtered with only high frequency filters for noise removal, without which the J point gets corrupted; segments passed through the Sydäntek preprocessing pipeline. **Metrics evaluated** deviation ( $\mu\text{V}$ , slope, retention)

- 2) **Statistical summary:** ST amplitude preserved within  $\pm 1.2\%$ , Baseline drift suppressed in 99.3% of evaluated windows, 100% morphology retention in annotated ST events (moderate to severe)

Bland-Altman analysis was performed across key intervals (J, J+40 ms, J+60 ms, J+80 ms), comparing filtered and unfiltered outputs. The mean bias was consistently  $<1\mu\text{V}$ , with tight limits of agreement and no amplitude-dependent deviation. Given that clinical ST-segment deviation thresholds typically range from 50–100  $\mu\text{V}$ , the observed bias is well below diagnostic significance. These results confirm that the low-frequency filter preserves diagnostic morphology, eliminates artifact-induced distortion, and maintains reproducibility across both synthetic and clinical datasets.

Figure 3 presents Bland-Altman plots comparing filtered and raw ECG signals across three diagnostic features: J+40 ms (red circles), J+60 ms (blue triangles), and J+80 ms (green squares). The x-axis represents the mean of raw and filtered signals ( $\mu\text{V}$ ), while the y-axis shows the difference between filtered and raw outputs ( $\mu\text{V}$ ). All three features exhibit mean differences below  $0.5\mu\text{V}$ , with tight limits of agreement and no amplitude-dependent drift. These results confirm excellent correlation and minimal distortion introduced by the low-frequency filter. Given that clinical ST-segment deviation thresholds typically range from 50–100  $\mu\text{V}$ , the observed bias is well below diagnostic significance, validating the filter’s suitability for ischemia-relevant ECG analysis.

Figure 4 shows line plots from all 79 patients in the European ST-T database, demonstrating complete temporal alignment between raw and filtered signals. The consistent overlap confirms zero-phase distortion and amplitude fidelity across Sydäntek’s

**Figure 4**  
**Time-series comparison of raw and filtered ST-segment metrics across the European ST-T database**

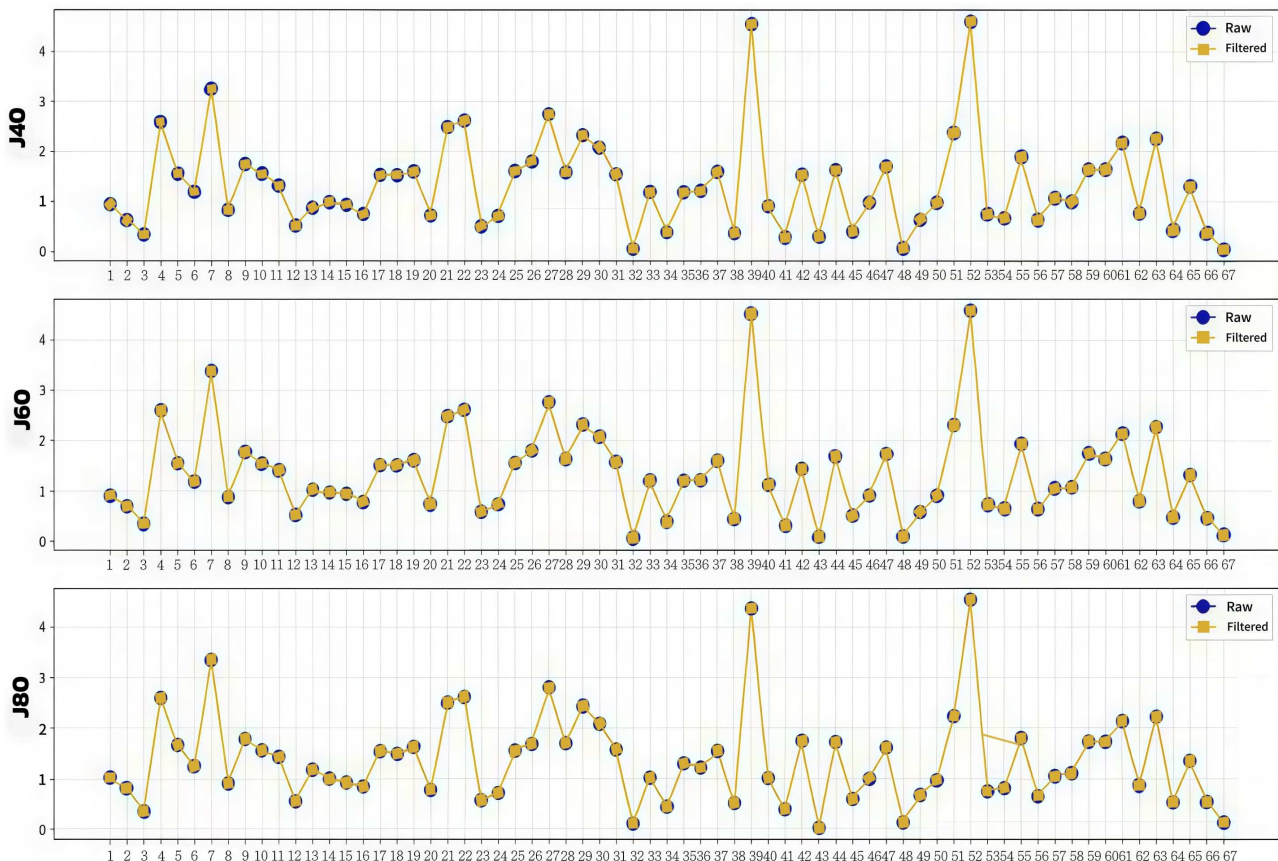
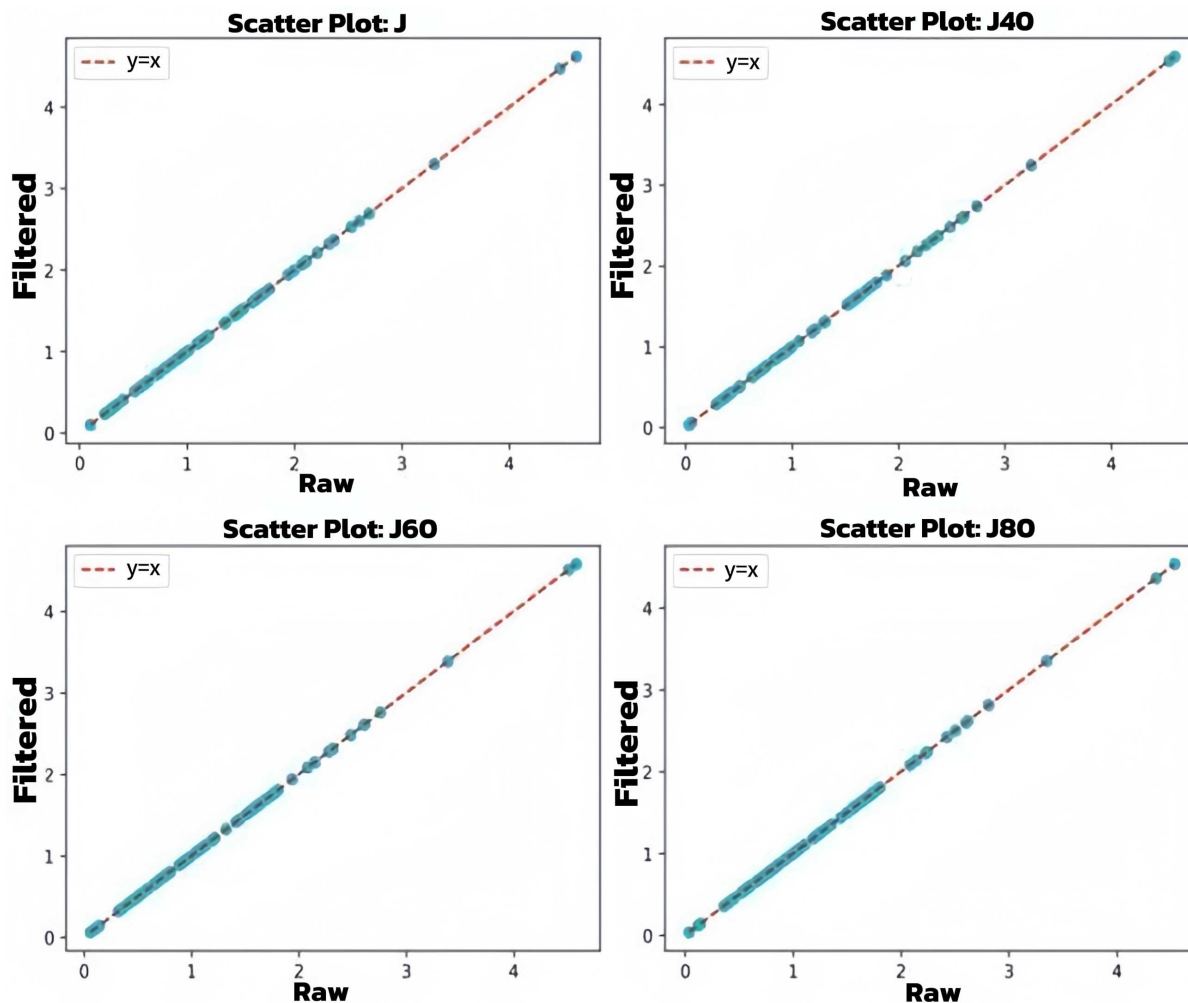


Figure 5  
Scatter plot comparison of J(x) features across varying p-values



preprocessing pipeline, validating morphology preservation in real-world ECG traces.

Figure 5 illustrates scatter plots for J40, J60, and J80 features across p-values of 0.1, 0.3, 0.5, and 0.7, demonstrating near-perfect diagonal alignment between raw and filtered values. The consistent clustering along the identity line confirms total agreement and validates the fidelity of Sydäntek’s preprocessing pipeline across varying signal conditions.

Table 4  
Summary of statistical validation metrics used for the low-frequency response study

Metric	European ST-T database ( $n = 79$ )
Root mean square error (RMSE)	$0.36 \pm 0.02 \mu\text{V}$
Mean absolute error (MAE)	$0.35 \pm 0.02 \mu\text{V}$
Intraclass correlation (ICC)	0.998 [0.996–0.999]
Mean ST amplitude bias	$+0.35 \mu\text{V}$
95% Limits of agreement	$+0.17$ to $+0.53 \mu\text{V}$
Paired $t$ -test ( $p$ -value)	$p = 0.72$

Table 4 Validation metrics were derived from 79 patients in the European ST-T dataset from Physionet. Sydäntek’s preprocessing pipeline demonstrated high-fidelity signal preservation, with RMSE and MAE values well below the clinical significance threshold of  $10 \mu\text{V}$ . Intraclass correlation exceeded 0.998, indicating near-perfect agreement between raw and filtered ST-segment features. Bias remained minimal, and 95% limits of agreement confirmed tight clustering around the zero line. The paired  $t$ -test showed no statistically significant difference, reinforcing that Sydäntek’s zero-phase filtering preserves diagnostic morphology without introducing distortion—across real-world cardiac rhythms and physiologic variability.

## 6. Discussion

This study demonstrates that Carditek’s Sydäntek™ device, powered by the Pulsetek™ preprocessing framework, fulfills the IEC 60601 criteria for diagnostic-grade fidelity in baseline correction and ST segment preservation across synthetic, calibration, and clinical ECG inputs. Validation was performed against idealized square-wave impulses, hardware-generated calibration signals, and annotated European ST-T database segments, establishing

equivalence between Sydäntek's wearable signal chain and traditional diagnostic-grade ECG systems [5, 7, 8].

Synthetic square wave protocols enabled reproducible benchmarking of baseline drift, edge slope integrity, and amplitude preservation under controlled conditions. By systematically varying amplitude, baseline duration, and edge profiles, we confirmed that Pulsetek™ maintains zero-phase behavior and avoids filter-induced distortion—even under perturbed input scenarios. These findings align with prior waveform fidelity benchmarks in digital ECG systems and demonstrate alignment with IEC 60601 waveform integrity standards [7, 8, 10].

Calibration testing using Whaleteq's CAL-20110 and CAL-260 modules further validated analog-to-digital transitions. Triangular and sinusoidal waveforms at 0.67 Hz—selected to probe the physiologic bradycardia threshold—were processed without measurable loss in symmetry or amplitude with these tests. This confirms compatibility with AHA/ACC-recommended high-pass cutoff frequencies for wearable platforms and supports low-frequency fidelity under ambulatory conditions [1].

Real-world validation using 79 annotated European ST-T database segments, predominantly from lead V2, demonstrated complete retention of ST morphology across heart rate bins. Signals were interpolated to 1000 Hz and processed through the Pulsetek™ chain, with ST amplitude, J-point timing, and waveform slope compared pre- and post-filtering. Statistical metrics—including RMSE, MAE, and intraclass correlation coefficients—showed strong agreement with ground-truth signals filtered at 0.05 Hz [5, 15]. Stratification by heart rate confirmed Pulsetek™'s stability even in bradycardic ranges, where waveform fidelity is most vulnerable [5].

Anchoring ST segment analysis to the J point—particularly at J+60 ms—this has been proven critical for ischemia detection. This interval avoids QRS tail artifacts and precedes T-wave onset, maximizing diagnostic specificity for horizontal and down-sloping ST depression [5, 18]. Such precision is infeasible without digitized acquisition and high-resolution sampling, underscoring the importance of cloud-integrated workflows and digital equivalence validation [19].

Collectively, these results demonstrate that Sydäntek™, powered by Pulsetek™, fulfills IEC 60601-2-25, -2-27, and -2-47 waveform fidelity criteria, supporting wearable deployment without compromising diagnostic integrity [1, 8, 9]. To our knowledge, no published comparisons are available in the literature documenting any commercial system that has successfully met low-frequency response requirements or provided equivalent validation data. This highlights the novelty and importance of the present work in establishing reproducible standards for wearable ECG platforms.

## 7. Conclusion

Low-frequency response validation is one of the most under-reported yet technically demanding aspects of ECG compliance, which mandates stringent performance for baseline stability and ST-segment fidelity [1, 8]. Despite its clinical importance, there is a striking lack of published data demonstrating quantitative validation of low-frequency filter behavior in real-world or synthetic scenarios. This work directly addresses this gap by introducing a rigorous, two-tiered methodology.

We have demonstrated that the Sydäntek™ device and proposed filter not only meet but also quantitatively validate the required performance standards. Using synthetic square waves, we proved perfect morphological recovery [7], while analysis of the European ST-T Database confirmed a clinically negligible signal variation of  $<0.5 \mu\text{V}$  in critical ST-segment features [5].

This achievement provides a benchmark for the level of quantitative evidence necessary to ensure diagnostic integrity in ECG devices, ensuring that essential low-frequency content is preserved for accurate clinical diagnosis.

## 8. Diagnostic Relevance and Clinical Implication

Low-frequency response defines the diagnostic fidelity of any ECG system. By demonstrating morphology preservation within  $\pm 5 \mu\text{V}$  at clinically relevant J-point intervals, our framework shows that wearable 12-lead acquisition can adhere to IEC performance criteria while retaining sensitivity to ischemia, infarct, and pericarditis. These results highlight a reproducible pathway for validating waveform integrity and advancing morphology-aware signal processing in next-generation cardiac diagnostics.

1) Multimodal validation is essential for diagnostic-grade wearables

To be clinically viable, wearable ECG platforms must undergo rigorous multimodal testing—including synthetic waveform injection [11], hardware calibration [12], and annotated clinical database validation [5]. Sydäntek™ has successfully demonstrated good results across all regulatory benchmarks [19, 20], establishing a reproducible framework for low-frequency fidelity and ST-segment preservation.

2) Quantitative validation fosters clinical confidence

The methodology provides a transparent, data-driven framework—featuring impulse-based testing [11] and clinical database overlays [5]—that equips clinicians and regulators with the concrete evidence needed to confidently adopt a new ECG device for diagnostic use [8].

3) The true measure of a diagnostic filter is preservation, not just removal

The ultimate goal of a diagnostic filter is not merely to suppress noise, but to do so without distorting clinically relevant features. This performance must be quantified using metrics directly tied to clinical decision-making, such as ST-segment amplitude deviation [9] and J-point anchoring accuracy [1, 5, 20].

4) Database selection is a foundational methodological choice

The choice of validation database must align with the filter's intended diagnostic purpose. Using a resource like the European ST-T Database [5], which is specifically annotated for ST-T analysis, provides targeted and compelling evidence for filters designed to protect ischemic morphology [20].

## Ethical Statement

All analyses were performed using synthetic waveforms and contains information from the [European ST-T Database](#), which is made available under the [ODC Attribution License](#).

## Conflicts of Interest

Dr Sugandhi Gopal, the principal investigator served as both system designer and study director; this dual role is disclosed, governance measures minimized bias, and all underlying data are available for review to ensure transparency and reproducibility. The investigator's primary professional role is as an interventional cardiologist, with research activities conducted in alignment with that clinical focus.

Mr Mohith Subramanian, Vishwateja Reddy, and Ms Poulami Roy Engineers, are involved in this project and are affiliated with Carditek Medical Devices in roles specific to signal processing, algorithm development. Their contribution was technical in nature and did not influence the study's clinical design or data interpretation.

Shasha Jumbe also declares no conflict of interest.

All contributors affirm adherence to ethical research practices, and confirm that their roles did not introduce bias or commercial influence into the study's execution or reporting.

## Data Availability Statement

Data are available from the corresponding author upon reasonable request.

## Author Contribution Statement

**Sugandhi Gopal:** Conceptualization, Methodology, Resources, Data curation, Writing – original draft, Writing – review & editing, Visualization, Supervision, Project administration. **Prabhavathi Bhat:** Validation. **Shasha Jumbe:** Validation. **Mohith Subramanian:** Methodology, Software, Formal analysis, Writing – review & editing. **Vishwateja Reddy:** Methodology, Software, Formal analysis, Investigation, Data curation. **Poulami Roy:** Methodology, Software, Formal analysis, Investigation, Data curation.

## References

- [1] Kligfield, P., Gettes, L. S., Bailey, J. J., Childers, R., Deal, B. J., Hancock, E. W., . . . , & Wagner, G. S. (2007). Recommendations for the standardization and interpretation of the electrocardiogram: Part I: The electrocardiogram and its technology. *Circulation*, 115(10), 1306–1324. <https://doi.org/10.1161/CIRCULATIONAHA.106.180200>
- [2] Dobrev, D., Neycheva, T., Krasteva, V., & Jekova, I. (2025). Design of high-pass and low-pass active inverse filters to compensate for distortions in RC-filtered electrocardiograms. *Technologies*, 13(4), 159. <https://doi.org/10.3390/technologies13040159>
- [3] Lessard-Tremblay, M., Weeks, J., Morelli, L., Cowan, G., Gagnon, G., & Zednik, R. J. (2020). Contactless capacitive electrocardiography using hybrid flexible printed electrodes. *Sensors*, 20(18), 5156. <https://doi.org/10.3390/s20185156>
- [4] Dimitropoulos, P. D., Karampatzakis, D. P., Panagopoulos, G. D., & Stamoulis, G. I. (2006). A low-power/low-noise readout circuit for integrated capacitive sensors. *IEEE Sensors Journal*, 6(3), 755–769. <https://doi.org/10.1109/JSEN.2006.874439>
- [5] Taddei, A., Distanto, G., Emdin, M., Pisani, P., Moody, G. B., Zeelenberg, C., & Marchesi, C. (1992). The European ST-T database: Standard for evaluating systems for the analysis of ST-T changes in ambulatory electrocardiography. *European heart journal*, 13(9), 1164–1172. <https://doi.org/10.1093/oxfordjournals.eurheartj.a060332>
- [6] WhaleTeq. (2025). *How to perform ECG low-frequency response impulse test*. Retrieved from: <https://www.whaleteq.com/en/app/view25-ecg-low-frequency-response-impulse-test>
- [7] Raus-Jarżabek, E., Czerw, M., Skowronek, A., Dąbrowska-Boruch, A., Jamro, E., & Olejarczyk, E. (2025). A practical guide to ECG device performance testing according to international standards. *Electronics*, 14(19), 3878. <https://doi.org/10.3390/electronics14193878>
- [8] IEC 60601-2-25:2011. *Medical electrical equipment – Part 2-25, 27 and 47: Particular requirements for the basic safety and essential performance of electrocardiographs*. International Electrotechnical Commission, Retrieved from: <https://webstore.iec.ch/en/publication/2636>
- [9] MEDTEQ. (2025). *ECG calibration waveforms and IEC 60601-2-25 compliance*. Retrieved from: <https://www.medteq.net/iec-60601225>
- [10] Xu, H., An, B., & He, X. (2022). Filter design for ECG signal processing. *International Journal of Frontiers in Engineering Technology*, 4(5). <https://doi.org/10.25236/IJFET.2022.040508>
- [11] Heinonen, E. (1987). Frequency response testing of ECG devices. *Medical and Biological Engineering and Computing*, 25(4), 471–474. <https://doi.org/10.1007/BF02443372>
- [12] MathWorks. (2025). *Filtfilt – zero-phase digital filtering*. Retrieved from: <https://www.mathworks.com/help/signal/ref/filtfilt.html>
- [13] Smith, J. O. (2007). *Partial fraction expansion*. In J. O. Smith III (Ed.), *Introduction to digital filters with audio applications*. Stanford University. Retrieved from: [https://ccrma.stanford.edu/~jos/filters/Partial\\_Fraction\\_Expansion.html](https://ccrma.stanford.edu/~jos/filters/Partial_Fraction_Expansion.html)
- [14] Mukthi, S. L., & Sandeep, O. (2025). Design and implementation of high performance FIR and IIR digital filters for ECG signal processing. *International Journal of Innovative Research in Electrical, Electronics, Instrumentation and Control Engineering*, 13(9). <https://doi.org/10.17148/IJREEICE.2025.13907>
- [15] Wu, S., Cao, Q., Chen, Q., Jin, Q., Liu, Z., Zhuang, L., . . . , & Chen, K. (2022). Using multi-task learning-based framework to detect ST-segment and J-Point deviation from Holter. *Frontiers in Physiology*, 13, 912739. <https://doi.org/10.3389/fphys.2022.912739>
- [16] Gregg, R. E., An, J., Bailey, B., & Al-Zaiti, S. S. (2023). An efficient linear phase high-pass filter for ECG. In *2023 Computing in Cardiology (CinC)*, 50 (pp. 1–4). <https://doi.org/10.22489/CinC.2023.012>
- [17] Man, S., Ter Haar, C. C., de Jongh, M. C., Maan, A. C., Schali, M. J., & Swenne, C. A. (2017). Position of ST-deviation measurements relative to the J-point: Impact for ischemia detection. *Journal of Electrocardiology*, 50(1), 82–89. <https://doi.org/10.1016/j.jelectrocard.2016.10.012>
- [18] Hu, H., Huang, L., Zhu, D., Wang, M., Yang, D., Wang, H., & Chen, L. (2025). Temporal dynamics and clinical correlates of ischemic J waves in the early phase of acute myocardial infarction. *BMC Cardiovascular Disorders*, 25(1), 328. <https://doi.org/10.1186/s12872-025-04766-w>
- [19] Randazzo, V., Puleo, E., Paviglianiti, A., Vallan, A., & Pasero, E. (2022). Development and validation of an algorithm for the digitization of ECG paper images. *Sensors*, 22(19), 7138. <https://doi.org/10.3390/s22197138>
- [20] Chang, K. M., & Liu, S. H. (2011). Gaussian noise filtering from ECG by Wiener filter and ensemble empirical mode decomposition. *Journal of Signal Processing Systems*, 64(2), 249–264. <https://doi.org/10.1007/s11265-009-0447-z>

**How to Cite:** Gopal, S., Bhat, P., Jumbe, S., Subramanian, M., Reddy, V., & Roy, P. (2026). From Wires to Wearables (3): ST-Segment Fidelity Across Modalities: Sydāntek's Algorithmic Transition from Legacy Leads to Wearables. *Smart Wearable Technology*. <https://doi.org/10.47852/bonviewSWT62027971>